Motion Planning of the Sit to Stand Movement for Powered Lower Limb Orthoses

Octavio Narvaez-Aroche
Andrew Packard
Murat Arcak

Electrical Engineering and Computer Sciences
University of California at Berkeley

Technical Report No. UCB/EECS-2017-148
http://www2.eecs.berkeley.edu/Pubs/TechRpts/2017/EECS-2017-148.html

August 11, 2017

Motion Planning of the Sit to Stand Movement for Powered Lower Limb Orthoses

Octavio Narváez-Aroche*, Prof. Andrew Packard*, Prof. Murat Arcak**
ocnaar@berkeley.edu, apackard@berkeley.edu, arcak@berkeley.edu

*Berkeley Center for Control and Identification, Department of Mechanical Engineering
**Department of Electrical Engineering and Computer Sciences
University of California, Berkeley, California, 94720

ABSTRACT

We propose a generalizable strategy for planning the sit to stand movement of a powered lower limb orthosis and its user. Modeling the system as a three rigid link planar robot, we rely on its kinematic equations to obtain a set of transformations that allows us to compute reference trajectories for the angular positions of the links, starting from a desired kinematic behavior for the center of mass of the robot and the angular position of link 2 relative to link 1; as we consider them more suitable to define for achieving a safe sit to stand transition. We then proceed to design a tracking controller via feedback linearization and solve a constrained least-squares program to address the control allocation problem from including the loads applied by the arms of the user as inputs. We simulate two relevant STS movements to illustrate the system tracking the reference trajectories generated with our strategy, in the presence of parameter uncertainty.

BACKGROUND

Wearable robots are complex biomechatronics systems that must work in synchrony with the body of its user in order to perform a mechanical task. They can be worn in series to replace missing extremities (powered prostheses), or in parallel to provide power augmentation or rehabilitation (powered orthoses) [1]. Powered lower limb orthoses are wearable robots designed as medical devices that aid the mobility and enhance the strength of the legs or their individual joints to assist standing and/or walking. We study a class of these orthoses (sometimes referred to as medical exoskeletons) whose purpose is to restore the gait of people with complete paralysis of the lower part of the body, by providing physical support and load transfer to the ground with externally coupled rigid links. Their users, who interact with the ground by means of crutches, must have good mobility in hands, arms, and shoulders; as well as healthy enough skeletal, cardiovascular, vestibular and visual systems to tolerate standing.

State of the art powered lower limb orthoses such as EksoGT [2], Indego [3], ReWalk [4] and Roki [5] provide actuation at the knees. In contrast, inspired by the gait of bilateral transfemoral amputees with passive knee prostheses [6], the Steven Exoskeleton (commercially available as PhoeniX [7]) has passive brake mechanisms at the knees and relies solely on the control of the motors at the hips to achieve adequate toe clearance for level ground walking. This architecture is a key feature to reduce mass, design complexity and ultimately cost [8].

The Sit to Stand (STS) movement is the sequence of actions that are executed for rising from a chair. Biomechanically, it is a complex activity that requires adequate position and torque control at each joint of the legs, precise spatial and temporal coordination of all body segments with feedback from the equilibrium sense [9], and can be more demanding than other activities of daily living because it requires more leg strength and greater ranges of joint motion than walking or stair climbing [10].

While powered lower limb orthoses without actuation at the knees allow dynamically stable gait cycles that look more natural when compared to fully-actuated ones, the trade off is that they demand more effort to perform the STS movement. Not only do the users need to compensate the lack of torque at the knees applying greater forces with their arms but they also find it more challenging to stabilize in the upright posture. This paper presents an approach to plan the motion of these devices, regarding the kinematics of the angular position of the thighs relative to the shanks and the Center of Mass (CoM) as good criteria to guarantee a safe transition from sitting to standing.

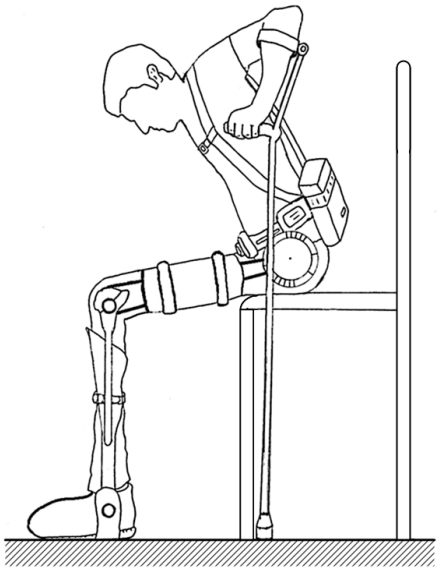

Figure 1: Representation of a subject about to perform a STS movement, assisted by a powered lower limb orthosis without actuation at the knees. Sagittal symmetry is assumed.

INTRODUCTION

Based on the evidence that three rigid link dynamic models have been used to accurately describe the STS movement of different subjects [11], we model the system comprised of a powered lower limb orthosis and its wearer as a three-link planar robot, where the interaction of the subject with the ground using crutches is represented by reactive loads acting on the location of the shoulder joints. The Euler-Lagrange equations for such system are compactly written in terms of the vector of joint angles θ, its time derivatives and input u as

$$\ddot{\theta} = f\left(\theta, \dot{\theta}, u\right)$$

Nevertheless, biomechanical studies measure the kinematics of the Center of Mass (CoM) to classify and assess dynamic balance of the STS movement [12] rather than joint angles. Therefore, we consider the angular position of the thighs relative to the shanks, θ_2, and the position coordinates of the CoM of the three-link planar robot in an intertial frame, (x_{CoM}, y_{CoM}), to define $z := \begin{bmatrix} \theta_2 & x_{CoM} & y_{CoM} \end{bmatrix}^T$ and show that a transformation of the form

$$\begin{bmatrix} \theta & \dot{\theta} & \ddot{\theta} \end{bmatrix}^T = h\left(z, \dot{z}, \ddot{z}\right) \tag{1}$$

can be obtained, in order to plan adequate STS movements in the space of z.

With the reference trajectories for the angular positions of the links and their first and second time derivatives, we proceed to design a tracking controller via feedback linearization of the Euler-Lagrange equations of the system. Due to our choice of inputs, this will also require to use a control allocation algorithm. To show the behaviour of the system under the proposed tracking nonlinear feedback controller, we present the simulation of two different STS movements designed with our motion planning approach, including uncertainties in the parameters of the system in order to perform a basic assessment of its robustness.

We only found one detailed STS motion planning and control algorithm for a comparable medical device in the literature, [13]. In contrast to our strategy, the STS movement of the Robot Suit HAL is planned in terms of the Center of Pressure (CoP), hip and knee angles. The reference trajectory of the knee is tuned from data of the motion of a healthy person, the desired CoP is fixed in front of the ankles and the reference for the hip is calculated online with measurements of the knee and ankle angles. The PD controller for the torques at the joints of the ankles, knees and hips does not assume sagital symmetry. A monitor can display the position of the CoP estimated with floor reaction force sensors, so that the wearer can better interact with parallel bars to cooperate with the suit.

THREE-LINK ROBOT MODEL FOR STS MOVEMENT

Assuming sagittal symmetry, no movement of the head relative to the torso, and that feet are fixed to the ground; we will model the dynamics of the system comprised of the user, crutches and orthosis in Figure 1 as those of the three-link planar

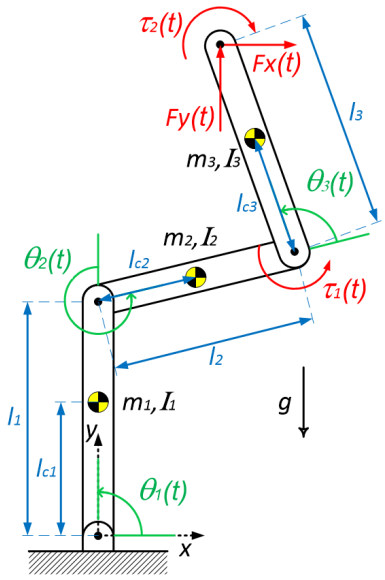

Figure 2: Three-link planar robot for modeling the powered lower limb orthosis and the interaction with its user.

robot with revolute joints coaxial to the ankles, knees and hips of the user, shown in Figure 2. The origin of the inertial frame is chosen at the joint of the ankles, $\theta_1(t)$ is the angular position of link 1 measured from the x axis at time t, $\theta_2(t)$ is the angular position of link 2 relative to link 1, and $\theta_3(t)$ is the angular position of link 3 relative to link 2. The length of link 1, l_1, is equal to the distance between the knees and the ankles, the length of link 2, l_2, is the distance between the knees and the hips and the length of link 3, l_3, is the distance between the hips and the shoulders, all of them measured in the sagittal plane. The mass of link 1, m_1, comprises the masses of the shanks of the user and the corresponding assemblies of the orthosis in that segment, the mass of link 2, m_2, is the mass of the thighs plus the components of the orthosis holding them, and the mass of link 3, m_3, includes the mass of the head, trunk and all parts of the orthosis attached to it. I_1, I_2 and I_3 are the moments of inertia of the links about their respective CoMs. The CoM of link 1 is a distance l_{c1} from the ankles, the CoM of link 2 is a distance l_{c2} from the knees and the CoM of link 3 is a distance l_{c3} from the hips. In addition to the weights of the links, there are four external loads acting on the robot: the actuators of the orthosis exert the torque $\tau_1(t)$ about the hips; while the torque $\tau_2(t)$, the horizontal force $F_x(t)$ and the vertical force $F_y(t)$ capture the inertial and gravitational forces of the arms and, most importantly, the loads applied on the shoulders of the user by its interaction with the ground when using the crutches. There is no torque applied at the knees in compliance with the class of orthoses under study.

For notational convenience, denote

$$\begin{aligned} c_i &:= \cos\theta_i(t) \\ c_{ij} &:= \cos\left(\theta_i(t) + \theta_j(t)\right) \\ c_{ijk} &:= \cos\left(\theta_i(t) + \theta_j(t) + \theta_k(t)\right) \end{aligned}$$

and similarly for sin.

EULER-LAGRANGE EQUATIONS OF THE THREE-LINK ROBOT

The standard equations of motion for the three-link planar robot described in the previous section were obtained by using the symbolic multibody dynamics package PyDy (short for Python Dynamics) [14]. In terms of the joint angles θ, input u,

$$\theta = \begin{bmatrix} \theta_1 & \theta_2 & \theta_3 \end{bmatrix}^T \qquad u = \begin{bmatrix} \tau_1 & \tau_2 & F_x & F_y \end{bmatrix}^T$$

and the constants

$$\begin{aligned} k_0 &:= (m_1 + m_2 + m_3)^{-1} & k_1 &:= l_{c1}m_1 + l_1 m_2 + l_1 m_3 \\ k_2 &:= l_{c2}m_2 + l_2 m_3 & k_3 &:= l_{c3}m_3 \end{aligned}$$

the Euler-Lagrange equations can be written as

$$M(\theta)\ddot{\theta} + F\left(\theta, \dot{\theta}\right) = A_\tau(\theta)\, u \tag{2}$$

where $M(\theta) \in \mathbb{R}^{3\times 3}$, $M(\theta) \succ 0$ is the symmetric mass matrix of the system with entries

$$\begin{aligned}
M_{11} &= I_1 + I_2 + I_3 + l_{c1}^2 m_1 + m_2\left(l_1^2 + 2l_1 l_{c2} c_2 + l_{c2}^2\right) \\
&\quad + m_3\left(l_1^2 + 2l_1 l_2 c_2 + 2l_1 l_{c3} c_{23} + l_2^2 + 2l_2 l_{c3} c_3 + l_{c3}^2\right) \\
M_{12} &= I_2 + I_3 + l_{c2} m_2 (l_1 c_2 + l_{c2}) \\
&\quad + m_3\left(l_1 l_2 c_2 + l_1 l_{c3} c_{23} + l_2^2 + 2l_2 l_{c3} c_3 + l_{c3}^2\right) \\
M_{13} &= I_3 + l_{c3} m_3 (l_1 c_{23} + l_2 c_3 + l_{c3}) \\
M_{22} &= I_2 + I_3 + l_{c2}^2 m_2 + m_3\left(l_2^2 + 2l_2 l_{c3} c_3 + l_{c3}^2\right) \\
M_{23} &= I_3 + l_{c3} m_3 (l_2 c_3 + l_{c3}) \\
M_{33} &= I_3 + l_{c3}^2 m_3
\end{aligned}$$

$F\left(\theta, \dot{\theta}\right) \in \mathbb{R}^3$ is the vector of energy contributions due to the acceleration of gravity $g = 9.81\,[m/s^2]$ and Coriolis forces

$$F\left(\theta, \dot{\theta}\right) = \Omega(\theta) \begin{bmatrix} \dot{\theta}_1^2 \\ \left(\dot{\theta}_1 + \dot{\theta}_2\right)^2 \\ \left(\dot{\theta}_1 + \dot{\theta}_2 + \dot{\theta}_3\right)^2 \end{bmatrix} + g \begin{bmatrix} k_1 c_1 + k_2 c_{12} + k_3 c_{123} \\ k_2 c_{12} + k_3 c_{123} \\ k_3 c_{123} \end{bmatrix}$$

with

$$\Omega(\theta) = \begin{bmatrix} l_1 (k_2 s_2 + k_3 s_{23}) & -k_2 l_1 s_2 + k_3 l_2 s_3 & -k_3 l_1 s_{23} - k_3 l_2 s_3 \\ l_1 (k_2 s_2 + k_3 s_{23}) & k_3 l_2 s_3 & -k_3 l_2 s_3 \\ l_1 k_3 s_{23} & k_3 l_2 s_3 & 0 \end{bmatrix}$$

$A_\tau(\theta) \in \mathbb{R}^{3\times 4}$ is the generalized forces matrix

$$A_\tau(\theta) = \begin{bmatrix} 0 & -1 & -l_1 s_1 - l_2 s_{12} - l_3 s_{123} & l_1 c_1 + l_2 c_{12} + l_3 c_{123} \\ 0 & -1 & -l_2 s_{12} - l_3 s_{123} & l_2 c_{12} + l_3 c_{123} \\ 1 & -1 & -l_3 s_{123} & l_3 c_{123} \end{bmatrix}$$

KINEMATICS OF THE CoM OF THE THREE-LINK ROBOT

In this section we show that a transformation of the form (1) can be found from the kinematic equations of the CoM of the three-link robot.

The position, velocity and acceleration coordinates of the CoM are

$$x_{CoM} = k_0 (k_1 c_1 + k_2 c_{12} + k_3 c_{123}) \tag{3}$$

$$y_{CoM} = k_0 (k_1 s_1 + k_2 s_{12} + k_3 s_{123}) \tag{4}$$

$$\dot{x}_{CoM} = -\dot{\theta}_1 y_{CoM} - \dot{\theta}_2 k_0 (k_2 s_{12} + k_3 s_{123}) - \dot{\theta}_3 k_0 k_3 s_{123} \tag{5}$$

$$\dot{y}_{CoM} = \dot{\theta}_1 x_{CoM} + \dot{\theta}_2 k_0 (k_2 c_{12} + k_3 c_{123}) + \dot{\theta}_3 k_0 k_3 c_{123} \tag{6}$$

$$\begin{aligned}
\ddot{x}_{CoM} &= -\dot{\theta}_1^2 x_{CoM} - \dot{\theta}_2^2 k_0 (k_2 c_{12} + k_3 c_{123}) - \dot{\theta}_3^2 k_0 k_3 c_{123} \\
&\quad - 2\dot{\theta}_1 \dot{\theta}_2 k_0 (k_2 c_{12} + k_3 c_{123}) - 2\left(\dot{\theta}_1 + \dot{\theta}_2\right) \dot{\theta}_3 k_0 k_3 c_{123} \\
&\quad - \ddot{\theta}_1 y_{CoM} - \ddot{\theta}_2 k_0 (k_2 s_{12} + k_3 s_{123}) - \ddot{\theta}_3 k_0 k_3 s_{123}
\end{aligned} \tag{7}$$

$$\begin{aligned}
\ddot{y}_{CoM} &= -\dot{\theta}_1^2 y_{CoM} - \dot{\theta}_2^2 k_0 (k_2 s_{12} + k_3 s_{123}) - \dot{\theta}_3^2 k_0 k_3 s_{123} \\
&\quad - 2\dot{\theta}_1 \dot{\theta}_2 k_0 (k_2 s_{12} + k_3 s_{123}) - 2\left(\dot{\theta}_1 + \dot{\theta}_2\right) \dot{\theta}_3 k_0 k_3 s_{123} \\
&\quad + \ddot{\theta}_1 x_{CoM} + \ddot{\theta}_2 k_0 (k_2 c_{12} + k_3 c_{123}) + \ddot{\theta}_3 k_0 k_3 c_{123}
\end{aligned} \tag{8}$$

From equations (3) and (4), the position vector of the CoM of the three-link robot can be expressed as a sum of three vectors whose geometric representation is shown in Figure 3.

$$\begin{aligned}
\begin{bmatrix} x_{CoM} \\ y_{CoM} \end{bmatrix} &= k_0 k_1 \begin{bmatrix} c_1 \\ s_1 \end{bmatrix} + k_0 k_2 \begin{bmatrix} c_{12} \\ s_{12} \end{bmatrix} + k_0 k_3 \begin{bmatrix} c_{123} \\ s_{123} \end{bmatrix} \\
&= r_1 + r_2 + r_3
\end{aligned} \tag{9}$$

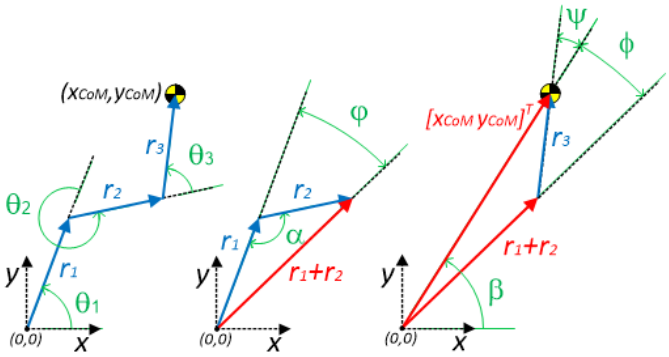

Figure 3: Geometric representation of vectors and angles used for expressing θ_1 and θ_3 as a function of (x_{CoM}, y_{CoM}) and θ_2.

According to the angles drawn in Figure 3, we can establish the following relationships

$$\begin{aligned} \alpha &= \theta_2 - \pi \\ \beta &= \arctan\left(\frac{y_{CoM}}{x_{CoM}}\right) \qquad (10) \\ \theta_1 &= \beta - \phi + \varphi \qquad (11) \\ \theta_3 &= \beta + \psi - (\theta_1 + \theta_2) \qquad (12) \end{aligned}$$

where for feasible and realistic STS movements (such as the ones studied in the following sections) $\phi \geq 0$ and $\varphi, \psi \in [-\pi/2, \pi/2]$.

From applying the law of cosines to the triangle formed by vectors $r_1 + r_2$, r_3, $\begin{bmatrix} x_{CoM} & y_{CoM} \end{bmatrix}^T$, and using the trigonometric identity $c_2 = c_{12}c_1 + s_{12}s_1$ we have

$$\begin{aligned} \phi(z) &= \arccos\left(\frac{\|r_3\|^2 - \|r_1 + r_2\|^2 - \left(x_{CoM}^2 + y_{CoM}^2\right)}{-2\|r_1 + r_2\|\sqrt{x_{CoM}^2 + y_{CoM}^2}}\right) \\ &= \arccos\left(\frac{(k_0 k_3)^2 - k_0^2\left(k_1^2 + k_2^2 + 2k_1k_2c_2\right) - \left(x_{CoM}^2 + y_{CoM}^2\right)}{-2k_0\sqrt{k_1^2 + k_2^2 + 2k_1k_2c_2}\sqrt{x_{CoM}^2 + y_{CoM}^2}}\right) \end{aligned}$$

From the law of sines for the triangle of vectors r_1, r_2 and $r_1 + r_2$ we know

$$\begin{aligned} \varphi(z) &= \arcsin\left(\frac{\|r_2\|\sin\alpha}{\|r_1 + r_2\|}\right) \\ &= \arcsin\left(\frac{k_2\sin(\theta_2 - \pi)}{\sqrt{k_1^2 + k_2^2 + 2k_1k_2c_2}}\right) \end{aligned}$$

$$\begin{aligned} \psi(z) &= \arcsin\left(\frac{\|r_1 + r_2\|\sin\phi(z)}{\|r_3\|}\right) \\ &= \arcsin\left(\frac{\sqrt{k_1^2 + k_2^2 + 2k_1k_2c_2}\sin\phi(z)}{k_3}\right) \end{aligned}$$

Plugging these expressions for β,ϕ, φ and ψ in equations (11) and (12), we define the transformation $h_1 : z \to \theta$

$$\begin{aligned} \theta &= \begin{bmatrix} \arctan\left(\frac{y_{CoM}}{x_{CoM}}\right) - \phi(z) + \varphi(z) \\ \theta_2 \\ \arctan\left(\frac{y_{CoM}}{x_{CoM}}\right) + \psi(z) - (\theta_1(z) + \theta_2) \end{bmatrix} \\ &=: h_1(z) \end{aligned}$$

It is important to note that this transformation relies on the triangulation of the vectors in equation (9), so it does not hold in the vertical position, when $\theta_1 = \pi/2$ and $\theta_2 = \theta_3 = 0$.

Let

$$\begin{aligned} V(z,\theta): &= \begin{bmatrix} -y_{CoM} & -k_0 k_3 s_{123} \\ x_{CoM} & k_0 k_3 c_{123} \end{bmatrix} \\ q\left(\theta,\dot{\theta},\dot{z}\right): &= -\begin{bmatrix} x_{CoM} & k_0\left(k_2 c_{12}+k_3 c_{123}\right) & k_0 k_3 c_{123} \\ y_{CoM} & k_0\left(k_2 s_{12}+k_3 s_{123}\right) & k_0 k_3 s_{123} \end{bmatrix} \begin{bmatrix} \dot{\theta}_1^2 \\ \dot{\theta}_2^2 \\ \dot{\theta}_3^2 \end{bmatrix} \\ &\quad -2\dot{\theta}_1\dot{\theta}_2 \begin{bmatrix} k_0\left(k_2 c_{12}+k_3 c_{123}\right) \\ k_0\left(k_2 s_{12}+k_3 s_{123}\right) \end{bmatrix} \\ &\quad -2\left(\dot{\theta}_1+\dot{\theta}_2\right)\dot{\theta}_3 \begin{bmatrix} k_0 k_3 c_{123} \\ k_0 k_3 s_{123} \end{bmatrix} \\ &\quad +\begin{bmatrix} -k_0\left(k_2 s_{12}+k_3 s_{123}\right) \\ k_0\left(k_2 c_{12}+k_3 c_{123}\right) \end{bmatrix} \ddot{\theta}_2 \end{aligned}$$

From equations (5) and (6), the velocity vector of the CoM of the three-link robot is

$$\begin{bmatrix} \dot{x}_{CoM} \\ \dot{y}_{CoM} \end{bmatrix} = \dot{\theta}_2 \begin{bmatrix} -k_0\left(k_2 s_{12}+k_3 s_{123}\right) \\ k_0\left(k_2 c_{12}+k_3 c_{123}\right) \end{bmatrix} + V\left(z,h_1(z)\right)\begin{bmatrix} \dot{\theta}_1 \\ \dot{\theta}_3 \end{bmatrix}$$

$V\left(z,h_1(z)\right)$ is singular if $\theta_1+\theta_2+\theta_3 = \arctan\left(\frac{y_{CoM}}{x_{CoM}}\right)$, and according to expressions (10) and (12) this condition will hold iff $\psi = 0$; which requires vectors r_1+r_2 and r_3 to be aligned. In the case of feasible and realistic STS movements, this will only occur in the vertical position. For all other configurations, we calculate the angular velocities of links 1 and 3 as

$$\begin{aligned} \begin{bmatrix} \dot{\theta}_1 \\ \dot{\theta}_3 \end{bmatrix} &= V\left(z,h_1(z)\right)^{-1}\left(\begin{bmatrix} \dot{x}_{CoM} \\ \dot{y}_{CoM} \end{bmatrix} - \dot{\theta}_2 \begin{bmatrix} -k_0\left(k_2 s_{12}+k_3 s_{123}\right) \\ k_0\left(k_2 c_{12}+k_3 c_{123}\right) \end{bmatrix}\right) \\ &=: p\left(z,\dot{z}\right) \end{aligned}$$

so that a transformation $h_2 : z,\dot{z} \to \dot{\theta}$ is defined

$$\begin{aligned} \dot{\theta} &= \begin{bmatrix} 1 & 0 \\ 0 & 0 \\ 0 & 1 \end{bmatrix} p\left(z,\dot{z}\right) + \begin{bmatrix} 0 \\ \dot{\theta}_2 \\ 0 \end{bmatrix} \\ &=: h_2\left(z,\dot{z}\right) \end{aligned}$$

From equations (7) and (8), the acceleration vector of the CoM is

$$\begin{bmatrix} \ddot{x}_{CoM} \\ \ddot{y}_{CoM} \end{bmatrix} = q\left(h_1(z),h_2\left(z,\dot{z}\right),\ddot{z}\right) + V\left(z,h_1(z)\right)\begin{bmatrix} \ddot{\theta}_1 \\ \ddot{\theta}_3 \end{bmatrix}$$

Thus

$$\begin{bmatrix} \ddot{\theta}_1 \\ \ddot{\theta}_3 \end{bmatrix} = V^{-1}\left(z,h_1(z)\right)\left(\begin{bmatrix} \ddot{x}_{CoM} \\ \ddot{y}_{CoM} \end{bmatrix} - q\left(h_1(z),h_2\left(z,\dot{z}\right),\ddot{z}\right)\right)$$

and we can define the transformation $h_3 : z,\dot{z},\ddot{z} \to \ddot{\theta}$ as

$$\begin{aligned} \ddot{\theta} &= \begin{bmatrix} 1 & 0 \\ 0 & 0 \\ 0 & 1 \end{bmatrix} V^{-1}\left(z,h_1(z)\right)\left(\begin{bmatrix} \ddot{x}_{CoM} \\ \ddot{y}_{CoM} \end{bmatrix} - q\left(h_1(z),h_2\left(z,\dot{z}\right),\ddot{z}\right)\right) \\ &\quad + \begin{bmatrix} 0 & \ddot{\theta}_2 & 0 \end{bmatrix}^T \\ &=: h_3\left(z,\dot{z},\ddot{z}\right) \end{aligned}$$

For notational compactness, we use

$$h\left(z,\dot{z},\ddot{z}\right) := \begin{bmatrix} h_1(z) \\ h_2\left(z,\dot{z}\right) \\ h_3\left(z,\dot{z},\ddot{z}\right) \end{bmatrix} \tag{13}$$

to denote the transformation from z coordinates to θ coordinates.

REFERENCE TRAJECTORIES FOR THE STS MOVEMENT

The reference trajectories $\bar{z} = \left[\begin{array}{ccc} \bar{\theta}_2(t) & \bar{x}_{CoM}(t) & \bar{y}_{CoM}(t) \end{array} \right]^T$ in the z coordinates, on the interval $t \in [0, t_f]$, are parameterized as

$$\begin{aligned} \bar{\theta}_2(t) &= \bar{\theta}_2(0) + \left(\bar{\theta}_2(t_f) - \bar{\theta}_2(0)\right) \Phi_1(t, t_f) \\ \bar{x}_{CoM}(t) &= \bar{x}_{CoM}(0) + \left(\bar{x}_{CoM}(t_f) - \bar{x}_{CoM}(0)\right) \Phi_2(t, t_f) \\ \bar{y}_{CoM}(t) &= \bar{y}_{CoM}(0) + \left(\bar{y}_{CoM}(t_f) - \bar{y}_{CoM}(0)\right) \Phi_3(t, t_f) \end{aligned}$$

where $\Phi_i(t, t_f)$ with $i = 1, 2, 3$ are polynomial functions satisfying $\Phi_i(0, t_f) = 0$ and $\Phi_i(t_f, t_f) = 1$. This formulation is taken from [15]. Once $\dot{\bar{z}}$ and $\ddot{\bar{z}}$ are computed, substitution into the transformation (13) yields the reference trajectories in the θ coordinates $\left[\begin{array}{ccc} \bar{\theta}(t) & \dot{\bar{\theta}}(t) & \ddot{\bar{\theta}}(t) \end{array} \right]^T = h\left(\bar{z}(t), \dot{\bar{z}}(t), \ddot{\bar{z}}(t)\right)$.

FEEDBACK LINEARIZATION WITH CONTROL ALLOCATION

If the input u satisfies

$$\begin{aligned} A_\tau(\theta) u &= M(\theta)\left(-K_p\left(\theta - \bar{\theta}(t)\right) - K_d\left(\dot{\theta} - \dot{\bar{\theta}}(t)\right) + \ddot{\bar{\theta}}(t)\right) \\ &\quad + F\left(\theta, \dot{\theta}\right) \end{aligned} \tag{14}$$

then the dynamics described by $M(\theta)\ddot{\theta} + F\left(\theta, \dot{\theta}\right) = A_\tau(\theta) u$ result in a linear differential equation governing the tracking error of the form

$$\ddot{\theta} - \ddot{\bar{\theta}}(t) + K_d\left(\dot{\theta} - \dot{\bar{\theta}}(t)\right) + K_p\left(\theta - \bar{\theta}(t)\right) = 0$$

With the synthetic input $v(t)$, defined as

$$v(t) := -K_p\left(\theta - \bar{\theta}(t)\right) - K_d\left(\dot{\theta} - \dot{\bar{\theta}}(t)\right)$$

the feedback linearized [16] equations are $\ddot{\theta} - \ddot{\bar{\theta}}(t) = v(t)$. The gain matrices $K_p, K_d \in \mathbb{R}^{3\times 3}$ can be chosen from a LQR optimal gain for the system

$$\left[\begin{array}{c} \dot{\theta} - \dot{\bar{\theta}}(t) \\ \ddot{\theta} - \ddot{\bar{\theta}}(t) \end{array} \right] = \left[\begin{array}{cc} 0 & I_3 \\ 0 & 0 \end{array} \right] \left[\begin{array}{c} \theta - \bar{\theta}(t) \\ \dot{\theta} - \dot{\bar{\theta}}(t) \end{array} \right] + \left[\begin{array}{c} 0 \\ I_3 \end{array} \right] v(t)$$

which achieves asymptotically zero tracking error of the reference trajectories. For notational purposes define

$$\begin{aligned} b\left(t, \theta, \dot{\theta}\right) : &= M(\theta)\left(-K_p\left(\theta - \bar{\theta}(t)\right) - K_d\left(\dot{\theta} - \dot{\bar{\theta}}(t)\right) + \ddot{\bar{\theta}}(t)\right) \\ &\quad + F\left(\theta, \dot{\theta}\right) \end{aligned}$$

Since the system of equations (14) is underdetermined, at every time t we solve the control allocation [17] with the constrained least-squares program

$$\begin{aligned} u(t) = \quad & \underset{\xi}{\arg\min} && \frac{1}{2}\|W\xi\|_2^2 \\ & \text{subject to} && A_\tau(\theta(t))\,\xi = b\left(t, \theta(t), \dot{\theta}(t)\right) \\ & && lb \le \xi \le ub \end{aligned}$$

where $W \in \mathbb{R}^{3\times 3}$ and $lb, ub \in \mathbb{R}^4$ are user-specified weights and box constraints, respectively.

SIMULATION OF TWO STS MOVEMENTS

To illustrate the behaviour of the three-link robot system under the nonlinear feedback controller, we present results from the simulation of the system tracking two different STS movements in Figures 7 to 20. The dashed lines represent the evolution of the variables when the parameters of the system take the nominal values registered in Table 1. The collection of continuous

Table 1: Nominal Parameters of the System and their Uncertainties

Link	$m_i\ [kg]$	$I_i\ \left[kg \cdot m^2\right]$	$l_i\ [m]$	$l_{ci}\ [m]$
1	9.68 ± 0.1	1.16 ± 0.1	0.53 ± 0.01	$\frac{l_1}{2} \pm 0.01$
2	12.59 ± 0.1	0.52 ± 0.1	0.41 ± 0.01	$\frac{l_2}{2} \pm 0.01$
3	44.57 ± 0.1	2.56 ± 0.1	0.52 ± 0.01	$\frac{l_3}{2} \pm 0.01$

lines represent the evolution of the variables when the 12 parameters of the system are randomly chosen, within the domain of their uncertainties, by latin hypercube sampling of 200 experiments.

The first movement (STS 1) starts with the shank and torso segments parallel to the vertical, and the thigh segment parallel to the horizontal (Figure 4) setting $\theta_1(0) = 90^\circ$, $\theta_2(0) = -90^\circ$ and $\theta_3(0) = 90^\circ$ ($\overline{x}_{CoM}(0) = 0.309$ and $\overline{y}_{CoM}(0) = 0.6678$). The second movement (STS 2) vertically aligns the CoM and the ankle joint prior to seat-off (Figure 5) with the initial conditions $\theta_1(0) = 120^\circ$, $\theta_2(0) = -120^\circ$, $\theta_3(0) = 110.87^\circ$ ($\overline{x}_{CoM}(0) = 0$ and $\overline{y}_{CoM}(0) = 0.590$). For both movements, the final configuration of the system shown in Figure 6 places de CoM directly above the origin of the inertial frame with the values $\bar{\theta}_2(t_f) = -5^\circ$, $\overline{x}_{CoM}(t_f) = 0$ and $\overline{y}_{CoM}(t_f) = 0.974$. STS 1 and STS 2 are respectively referred in the biomechanical literature as dynamic and quasi-static strategies [9]. Most healthy people use the quasi-static strategy because it is safer and reduces the overall work; however, people with reduced knee strength tend to use a dynamic strategy. To complete the design of a rest-to-rest maneuver, define $\Phi_i(t, t_f) := -2\frac{t^3}{t_f^3} + 3\frac{t^2}{t_f^2}$, which is the only cubic polynomial satisfying $\dot{\Phi}(0, t_f) = \dot{\Phi}(t_f, t_f) = 0$ (and $\Phi(0, t_f) = 0$ and $\Phi(t_f, t_f) = 1$). Due to the lack of data on comfortable STS duration for subjects with complete spinal cord injuries, we picked one reported in [18] for stroke patients; leading to a simulation time of $t_f = 3.5\,[s]$ for both movements.

In this study the LQR weight matrices are $Q := I_6$ and $R := \frac{1}{100} I_3$. When solving the control allocation problem, we want to reflect that the contributions from the torque at the hips $\tau_1(t)$, the torque at the shoulders $\tau_2(t)$ and the vertical force $F_y(t)$ outweigh the horizontal force $F_x(t)$; we do this by considering the matrix $W = diag\left(\begin{bmatrix} 1 & 1 & 10 & 1 \end{bmatrix}\right)$ and, because the user always pushes the crutches down to propel upwards, we specify the constraint $F_y(t) \geq 0$. All other inputs are unconstrained.

We plan the STS motion in the z space instead of the θ space because it is not apparent how one would naturally arrive at the θ_1 and θ_3 trajectories shown in Figures 11 and 13. By contrast the trivial cubic expressions that define the reference trajectories in Figures 7, 8 and 12 are very natural, merely connecting starting and final points with zero slope boundary conditions. This is the prime motivation for having derived the transformation (13).

Because the controller operates with the nominal values of the parameters, the deviation of the the solid curves in Figures 7 to 16 from the reference trajectories was expected; nevertheless, it is a positive feature of the controller to find that the observed offsets do not lead to sit-back or step failures [11] nor to a condition of hyperextension of the knees, since all trajectories end in a small neighborhood of the final desired state and keep $\theta_2(t) \leq 0$. Based solely on the observed variance from the reference trajectories, STS 2 appears to be more sensitive to parameter uncertainty than STS 1, this is more noticeable in figure 9.

From Figures 17 to 20, we can tell that STS 1 significantly reduces $F_y(t)$ when compared to STS 2, which in turn requires a greater magnitude of $\tau_1(t)$. The values of $F_x(t)$ differ by one order of magnitude from $F_y(t)$ and remain within approximmately the same range in both movements, what is also observed for $\tau_2(t)$. It is interesting to see that while $F_y(t)$ for every STS 2 trajectory decreases from a maximum value observed at lift off, STS 1 trajectories peak over the period $t \in [0.75, 2.25]$.

CONCLUSIONS AND FURTHER WORK

From the conducted simulations, our STS motion planning strategy in the z space reduces the task to only choosing initial and final points with zero slope boundary conditions. Although the proposed feedback linearization controller achieves acceptable tracking errors in the presence of parameter uncertainties, the high sensitivity in the variability of $\tau_2(t)$, $F_x(t)$ and $F_y(t)$ demands a more careful study of its robustness; especially because these represent actions that must be performed by the user for successfully completing the movements and there is no feedback control/computer authority over them. A key concern is to enhance the control of $\tau_1(t)$ for making the system less sensitive to upper body loads.

The motion planning and control approaches of this paper focused on powered lower limb orthosis without actuation at the knees, but the same ideas could be extended to control fully actuated ones by applying the proper changes in the generalized forces matrix $A_\tau(\theta)$ and the control allocation program.

Our current feedback approach has an explicit time dependance on the reference trajectories; however, in practice, the

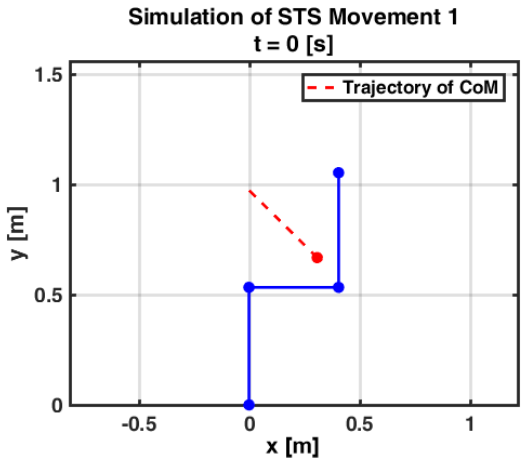

Figure 4: Initial position for STS 1. The dashed line represents the reference trajectory in the xy plane for the CoM.

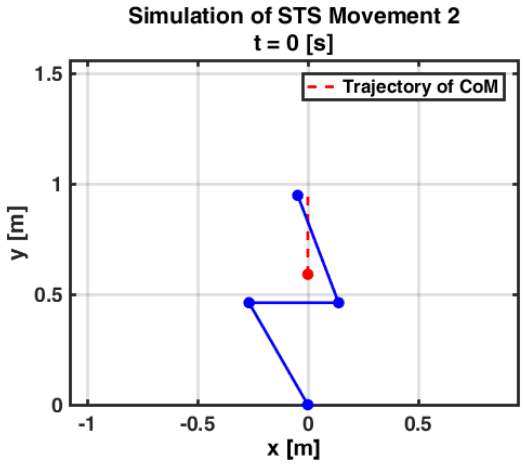

Figure 5: Initial position for STS 2. The dashed line represents the reference trajectory in the xy plane for the CoM.

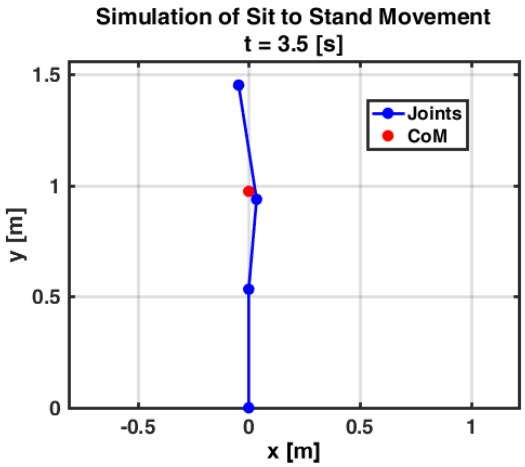

Figure 6: Final position for both STS movements.

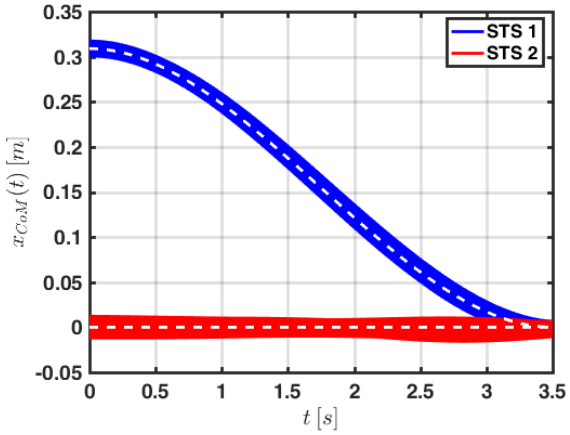

Figure 7: x axis coordinate of the three-link robot CoM.

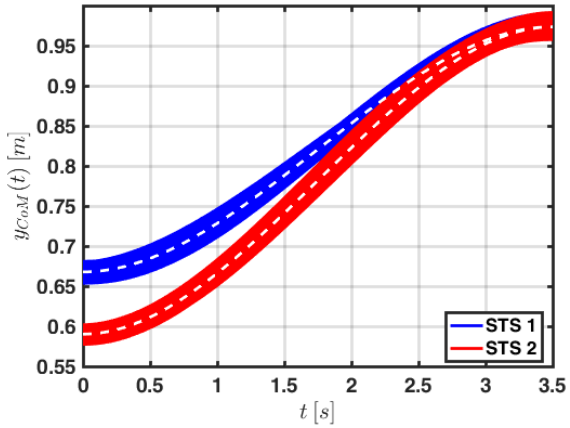

Figure 8: y axis coordinate of the three-link robot CoM.

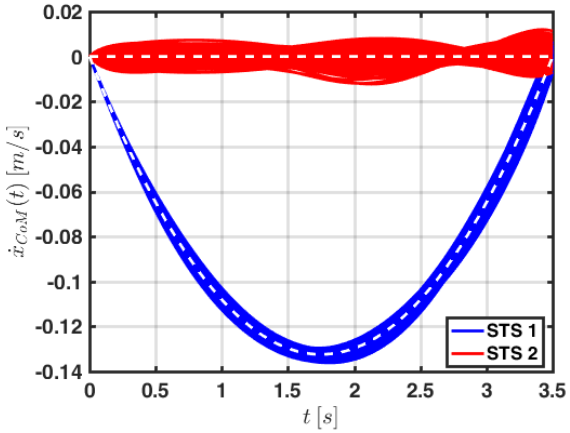

Figure 9: x axis coordinate of the velocity of the three-link robot CoM.

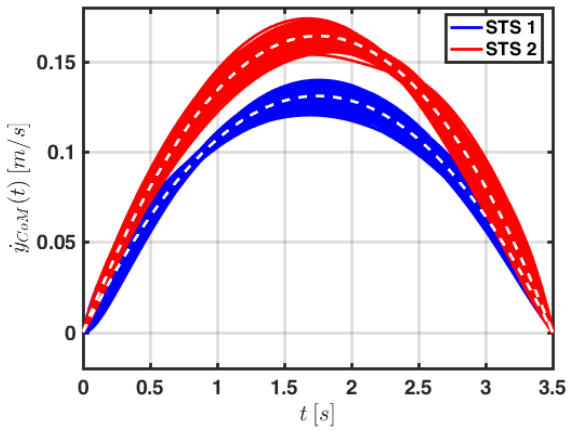

Figure 10: y axis coordinate of the velocity of the three-link robot CoM.

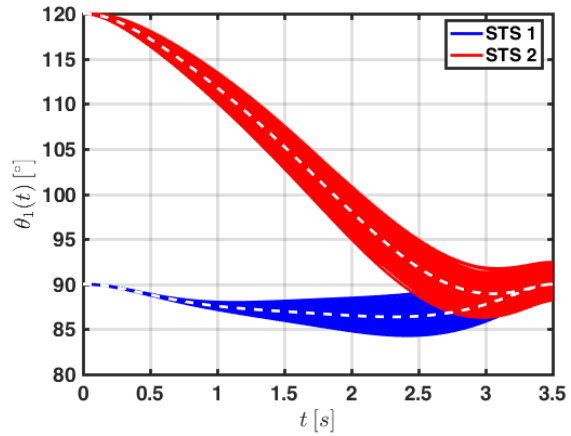

Figure 11: Angular position of link 1 relative to the horizontal.

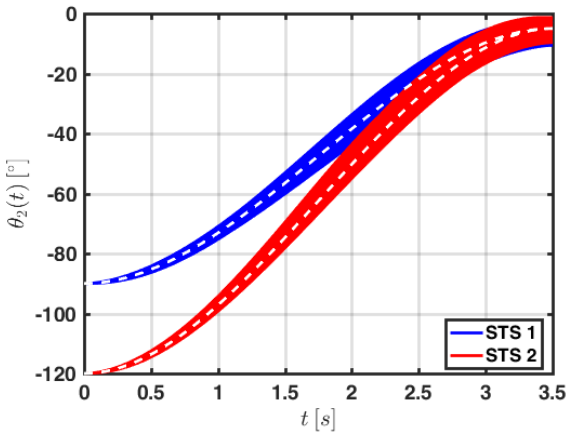

Figure 12: Angular position of link 2 relative to link 1.

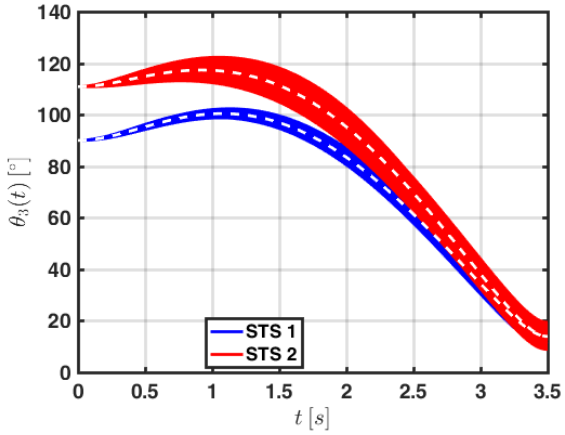

Figure 13: Angular position of link 3 relative to link 2.

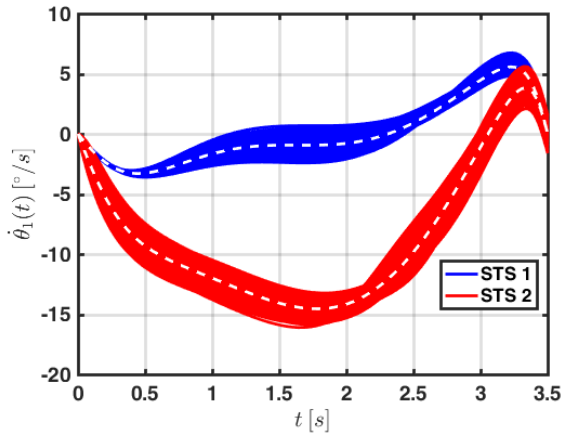

Figure 14: Angular velocity of link 1.

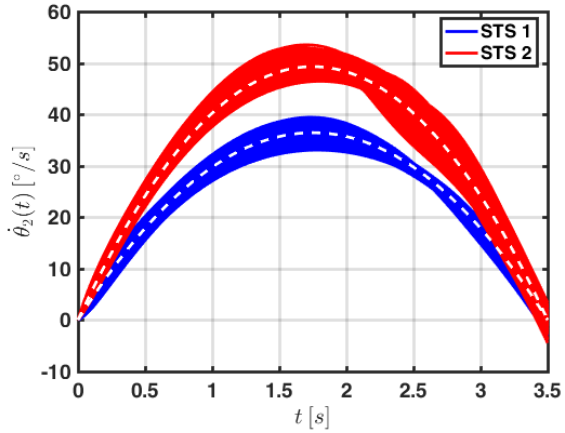

Figure 15: Angular velocity of link 2.

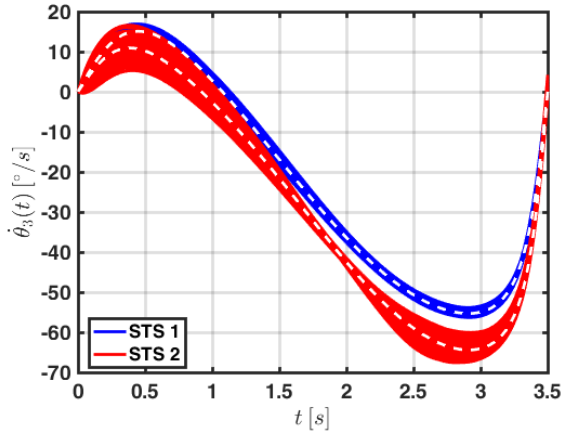

Figure 16: Angular velocity of link 3.

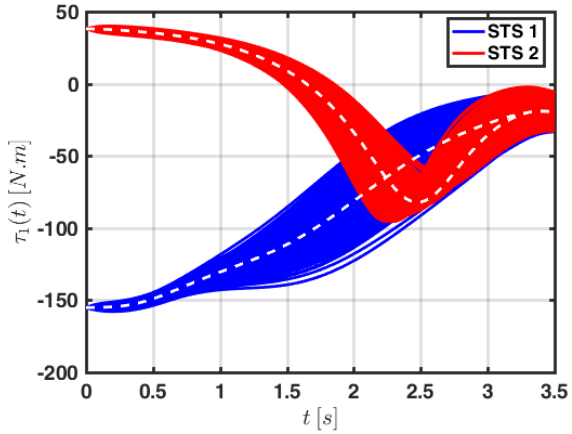

Figure 17: Torque applied at the hips by the powered lower limb orthosis.

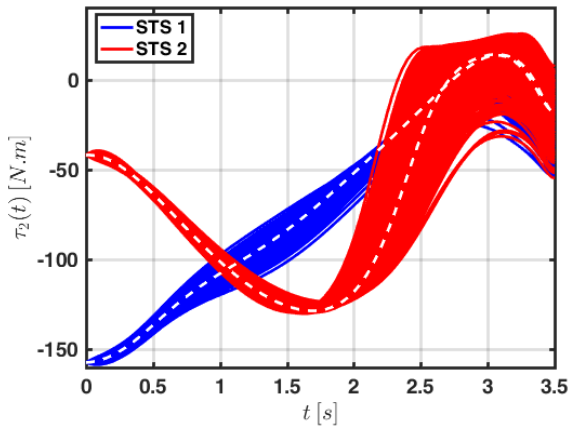

Figure 18: Torque at the shoulders of the user.

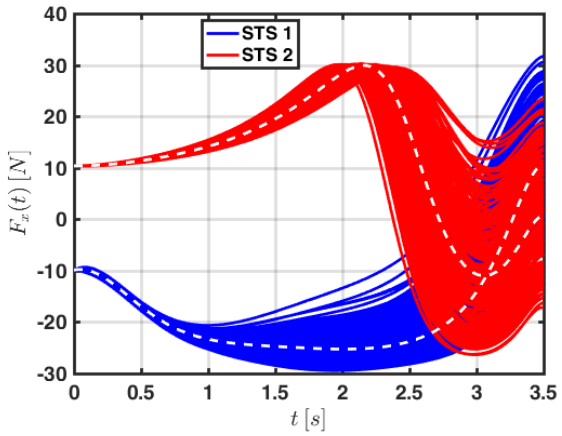

Figure 19: Horizontal force at the shoulders of the user.

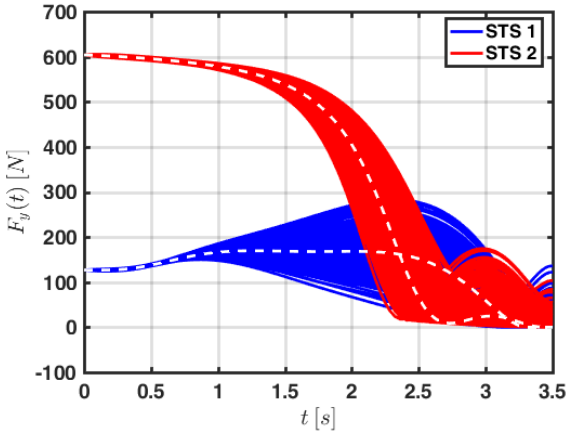

Figure 20: Vertical force at the shoulders of the user.

user of an orthosis might pause or act at a different time scale, which motivates path dependant controllers such as that proposed in [19]. In order to make our model more realistic, we also aim to add more links to represent the arms of the user and crutches.

ACKNOWLEDGEMENTS

The first author would like to thank the Consejo Nacional de Ciencia y Tecnologia (CONACYT), the Fulbright-Garcia Robles program and the University of California Institute for Mexico and the United States (UC MEXUS) for the scholarships that have made possible his Ph.D. studies; Dr. Maria Vrakopoulou for the artwork in Figure 1; and Professor J. Karl Hedrick, who first introduced him to feedback linearization.

The authors gratefully acknowledge the support from the National Science Foundation under grant ECCS-1405413 and the generous support from the FANUC Coorporation.

References

[1] Vertechy, R., and Accoto, D., 2014. "Wearable Robotics". *IEEE Robotics & Auto. Mag.,* **21**(4), pp. 19-20.

[2] Ekso Bionics, 2017. "EksoGT", from http://eksobionics.com/eksohealth/products/

[3] Parker Hannifin Corp, 2017. "Indego", from http://www.indego.com/indego/en/home

[4] ReWalk Robotics, 2017. "ReWalk More than Walking", from http://rewalk.com/

[5] Roki Robotics, 2017. "An Exo Created For You", from http://pro031jet.wixsite.com/roki

[6] McKinley, M. G., 2014. "Design of Lightweight Assistive Exoskeletons for Individuals with Mobility Disorders", Ph.D. thesis, UC Berkeley, CA. pp. 46-48.

[7] Exoskeleton Report LLC, 2017. "PhoeniX", from http://exoskeletonreport.com/product/phoenix/

[8] Strickland, E., 2016. "To Build the Best Robotic Exoskeleton, Make It on the Cheap", from http://spectrum.ieee.org/the-human-os/biomedical/bionics/to-build-the-fanciest-robotic-exoskeleton-make-it-on-the-cheap

[9] Galli, M., et. al., 2008. "Qualitative Analysis of Sit to Stand Movement: Experimental Set-up Definition and Application to Healthy and Hemiplegic Adults". *Gait and Posture,* **28**(1), pp. 80-85.

[10] Hughes, M. A., and Schenkman, M. L., 1996. "Chair Rise Strategy in the Functionally Impaired Elderly". *Journal of Rehabilitation Res. and Dev.,* **33**(4), pp. 409-412.

[11] Eby, W. R., and Kubica, E., 2006. "Modeling and Control Considerations for Powered Lower-Limb Orthoses: A Design Study for Assisted STS". *ASME Journal of Medical Devices,* **1**(2), pp. 126-139.

[12] Fujimoto, M., and Chou, L., 2012. "Dynamic balance control during sit-to-stand movement: An examination with the center of mass acceleration". *Journal of Biomechanics,* **45**, pp. 543-548.

[13] Tsukahara, A., Kawanishi, R., Hasegawa, Y., & Sankai, Y., 2010. "Sit-to-Stand and Stand-to-Sit Transfer Support for Complete Paraplegic Patients with Robot Suit HAL". *Advanced Robotics,* **24**(11), pp. 1615-1638.

[14] Gede, G., Peterson, D. L., Nanjangud, A. S., Moore, J. K., and Hubbard, M., 2013. "Constrained Multibody Dynamics With Python: From Symbolic Equation Generation to Publication". *9th International Conference on Multibody Systems, Nonlinear Dynamics, and Control.*

[15] Sira-Ramirez, H., and Agrawal, S. K., 2004. *Diferentially Flat Systems.* Marcel Dekker Inc, Control Engineering Series, New York, p.55 Chap. 2.

[16] Isidori, A., 1995. *Nonlinear Control Systems.* Springer-Verlag, London. pp. 219-291. Chap. 2.

[17] Johansen, T. A., and Fossen, T. I., 2013. "Control Allocation-A Survey". *Automatica*, **49**(5), pp. 1087-1103.

[18] Janssen, W. G., Bussmann, J. B., Horemans, H. L., and Stam, H. J., 2008. "Validity of Accelerometry in Assessing the Duration of the Sit-to-Stand Movement". *Journal of the International Federation for Medical & Biological Engineering & Computing*, **46**(9), pp. 879–887.

[19] Hauser, J., and Hindman, R., 1995. "Maneuver Regulation from Trajectory Tracking: Feedback Linearizable Systems". *Proceedings of IFAC Symposium on Nonlinear Control Systems Design,* pp. 595-600.